

EUROPEAN ORGANIZATION FOR NUCLEAR RESEARCH (CERN)



CERN-PH-EP-2014-223

LHCb-PAPER-2014-051

September 16, 2014

Measurement of the CP -violating phase ϕ_s in $\bar{B}_s^0 \rightarrow D_s^+ D_s^-$ decays

The LHCb collaboration[†]

Abstract

We present a measurement of the CP -violating weak mixing phase ϕ_s using the decay $\bar{B}_s^0 \rightarrow D_s^+ D_s^-$ in a data sample corresponding to 3.0 fb^{-1} of integrated luminosity collected with the LHCb detector in pp collisions at centre-of-mass energies of 7 and 8 TeV. An analysis of the time evolution of the system, which does not use the constraint $|\lambda| = 1$ to allow for the presence of CP violation in decay, yields $\phi_s = 0.02 \pm 0.17\text{ (stat)} \pm 0.02\text{ (syst)} \text{ rad}$, $|\lambda| = 0.91^{+0.18}_{-0.15}\text{ (stat)} \pm 0.02\text{ (syst)}$. This result is consistent with the Standard Model expectation.

Submitted to Phys. Rev. Lett.

© CERN on behalf of the LHCb collaboration, license CC-BY-4.0.

[†]Authors are listed at the end of this Letter.

The CP -violating weak mixing phase ϕ_s can be measured in the interference between mixing and decay of \bar{B}_s^0 mesons to CP eigenstates that proceeds via the $b \rightarrow c\bar{c}s$ transition, and is predicted to be small in the Standard Model (SM): $\phi_s^{\text{SM}} \approx -2\beta_s \equiv -2 \arg \left(-\frac{V_{ts}V_{tb}^*}{V_{cs}V_{cb}^*} \right) = -36.3^{+1.6}_{-1.5}$ mrad [1]. Measurements of ϕ_s are sensitive to the effects of potential non-SM particles contributing to the B_s^0 - \bar{B}_s^0 mixing amplitude. Several measurements of ϕ_s have been made with the decay mode $\bar{B}_s^0 \rightarrow J/\psi\phi$, with the first results showing tension with the SM expectation [2, 3]. Since then, more recent measurements of ϕ_s have found values consistent with the SM prediction in $\bar{B}_s^0 \rightarrow J/\psi K^+K^-$ and $\bar{B}_s^0 \rightarrow J/\psi\pi^+\pi^-$ decays [4–8]. The world average value determined prior to the publication of Ref. [5] is $\phi_s = 0 \pm 70$ mrad [9].

Precise measurements of ϕ_s are complicated by the presence of loop (penguin) diagrams, which could have an appreciable effect [10]. It is therefore important to measure ϕ_s in additional decay modes where penguin amplitudes may differ [11]. Additionally, in the $\bar{B}_s^0 \rightarrow J/\psi\phi$ channel, where a spin-0 meson decays to two spin-1 mesons, an angular analysis is required to disentangle statistically the CP -even and CP -odd components. The decay $\bar{B}_s^0 \rightarrow D_s^+D_s^-$ is also a $b \rightarrow c\bar{c}s$ transition with which ϕ_s can be measured [12], with the advantage that the $D_s^+D_s^-$ final state is CP -even, and does not require angular analysis.

In this Letter, we present the first measurement of ϕ_s in $\bar{B}_s^0 \rightarrow D_s^+D_s^-$ decays using an integrated luminosity of 3.0 fb^{-1} , obtained from pp collisions collected by the LHCb detector. One third of the data were collected at a centre-of-mass energy of 7 TeV , and the remainder at 8 TeV . We perform a fit to the time evolution of the \bar{B}_s^0 - B_s^0 system in order to extract ϕ_s .

LHCb is a single-arm forward spectrometer at the LHC designed for the study of particles containing b or c quarks in the pseudorapidity range 2 to 5 [13]. Events are selected by a trigger consisting of a hardware stage that identifies high transverse energy particles, followed by a software stage, which applies a full event reconstruction [14]. A multivariate algorithm [15] is used to select candidates with secondary vertices consistent with the decay of a b hadron.

Signal $\bar{B}_s^0 \rightarrow D_s^+D_s^-$ candidates are reconstructed in four final states: (i) $D_s^+ \rightarrow K^+K^-\pi^+$, $D_s^- \rightarrow K^-K^+\pi^-$; (ii) $D_s^+ \rightarrow K^+K^-\pi^+$, $D_s^- \rightarrow \pi^-\pi^+\pi^-$; (iii) $D_s^+ \rightarrow K^+K^-\pi^+$, $D_s^- \rightarrow K^-\pi^+\pi^-$; and (iv) $D_s^+ \rightarrow \pi^+\pi^-\pi^+$, $D_s^- \rightarrow \pi^-\pi^+\pi^-$. Inclusion of charge-conjugate processes, unless otherwise specified, is implicit. The $B^0 \rightarrow D^-D_s^+$ decay mode, where $D^- \rightarrow K^+\pi^-\pi^-$, and $D_s^+ \rightarrow K^+K^-\pi^+$, is used as a control channel. The selection requirements follow Ref. [16], apart from minor differences in the particle identification requirements and $B_{(s)}$ candidate mass regions. $D_{(s)}$ meson candidates are required to have masses within $25 \text{ MeV}/c^2$ of their known values [17] and to have a significant separation from the $B_{(s)}$ vertex. As the signatures of b -hadron decays to double-charm final states are all similar, vetoes are employed to suppress the cross-feed resulting from particle misidentification, following Ref. [18]. All $B_{(s)}$ candidates are refitted, taking both $D_{(s)}$ mass and vertex constraints into account [19]. A boosted decision tree (BDT) [20, 21] is used to improve the signal to background ratio. The BDT is trained with simulated decays to emulate the signal, and same-charge $D_s^+D_s^+$ and $D^+D_s^+$ from candidates with masses on the range

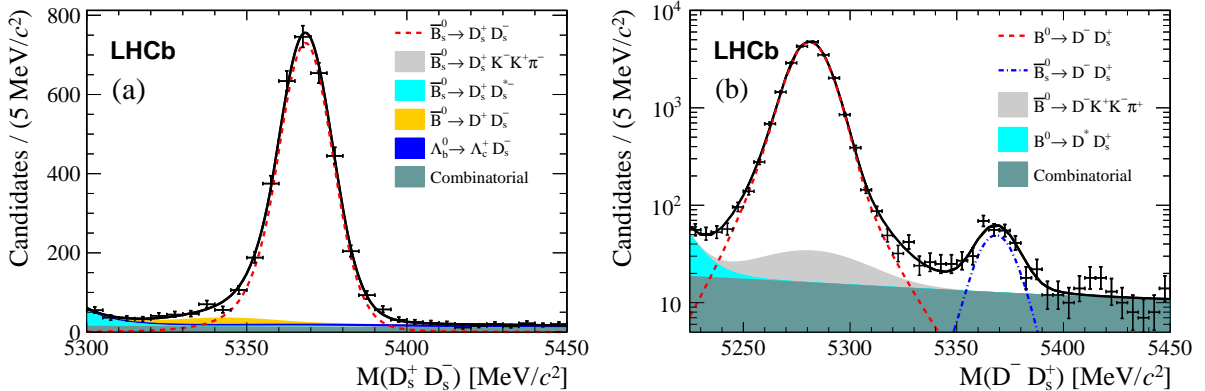


Figure 1: Invariant mass distributions of (a) $\bar{B}_s^0 \rightarrow D_s^+ D_s^-$ and (b) $B^0 \rightarrow D^- D_s^+$ candidates. The points show the data; the individual fit components are indicated in the legend; the black curve shows the overall fit.

$5200 < M(D_s^+ D_s^-) < 5650 \text{ MeV}/c^2$ and $5200 < M(D^- D_s^+) < 5600 \text{ MeV}/c^2$, respectively. The selection requirement on the BDT output, which retains about 98% of the signal events, is chosen to minimise the expected relative uncertainty in the $\bar{B}_s^0 \rightarrow D_s^+ D_s^-$ yield. The $B_{(s)}$ candidates are required to lie in the mass regions $5300 < M(D_s^+ D_s^-) < 5450 \text{ MeV}/c^2$ for the signal and $5200 < M(D^- D_s^+) < 5450 \text{ MeV}/c^2$ for the control channel, where the lower bound is chosen to suppress background contributions from $B_{(s)}$ decays with excited charm mesons in the final state. The decay time distribution is fitted in the range $0.2 < t < 12.0 \text{ ps}$ where the lower bound is chosen to reduce backgrounds from particles originating from the primary vertex.

The mass distributions for the signal, summed over the four final states, and the control channel are shown in Fig. 1, with results of unbinned maximum likelihood fits overlaid. The signal shapes are parameterised by the sum of two asymmetric Gaussian functions with a common mean. The background shapes are obtained from simulation [22–25]. Background rates from misidentified particles are obtained from $D^{*+} \rightarrow D^0 \pi^+$, $D^0 \rightarrow K^- \pi^+$ calibration data. Signal and background components are described in Ref. [16]. All yields in the fits to the full data sample are allowed to vary, except that corresponding to $\bar{B}_{(s)}^0 \rightarrow D_{(s)}^+ K^- K^+ \pi^-$ decays, which is fixed to be 1% of the signal yield as determined from a fit to the D_s mass sidebands. We observe 3345 ± 62 $\bar{B}_s^0 \rightarrow D_s^+ D_s^-$ signal and $21\,320 \pm 148$ $B^0 \rightarrow D^- D_s^+$ control channel decays. In the $D^- D_s^+$ channel, we also observe a contribution from $\bar{B}_s^0 \rightarrow D_s^+ D^-$ as reported previously [18]. We use the *sPlot* technique [26] to obtain the decay time distribution of $\bar{B}_s^0 \rightarrow D_s^+ D_s^-$ signal decays where the $D_s^+ D_s^-$ invariant mass is the discriminating variable. A fit to the background-subtracted distribution of the decay time, t , is performed using the signal-only decay time probability density function (PDF). The negative log likelihood to be minimised is

$$-\ln \mathcal{L} = -\alpha \sum_i^N W_i \ln \mathcal{P}(t_i, \delta_i, q_i^{\text{tag}} | \eta_i^{\text{tag}}), \quad (1)$$

where N denotes the total number of signal and background candidates in the fit region, W_i is the signal component weight and $\alpha = \sum_i^N W_i / \sum_i^N W_i^2$ [27]. The invariant mass is not correlated with the reconstructed decay time or its uncertainty, nor with flavour tagging output, for signal and background. The signal PDF, \mathcal{P} , includes detector resolution and acceptance effects and requires knowledge of the B_s^0 (\bar{B}_s^0) flavour at production,

$$\mathcal{P}(t, \delta, q^{\text{tag}} | \eta^{\text{tag}}) = R(\hat{t}, q^{\text{tag}} | \eta^{\text{tag}}) \otimes G(t - \hat{t} | \delta) \times \epsilon_{\text{data}}^{D_s^+ D_s^-}(t), \quad (2)$$

where \hat{t} is the decay time in the absence of resolution effects, $R(\hat{t}, q^{\text{tag}} | \eta^{\text{tag}})$ describes the rate including imperfect knowledge of the initial (\bar{B}_s^0) flavour through the flavour tag, q^{tag} , and the wrong-tag probability estimate η^{tag} . The flavour tag, q^{tag} , is -1 for \bar{B}_s^0 , $+1$ for B_s^0 and zero for untagged candidates. The calibrated decay time resolution is $G(t - \hat{t} | \delta)$ where δ is the decay time error estimate, and $\epsilon_{\text{data}}^{D_s^+ D_s^-}(t)$ is the decay time acceptance.

Allowing for CP violation in decay, the decay rates of (\bar{B}_s^0) mesons ignoring detector effects can be written as

$$\Gamma(\hat{t}) = \mathcal{N} e^{-\Gamma_s \hat{t}} \left[\cosh\left(\frac{\Delta\Gamma_s}{2}\hat{t}\right) - \frac{2|\lambda| \cos \phi_s}{1 + |\lambda|^2} \sinh\left(\frac{\Delta\Gamma_s}{2}\hat{t}\right) + \frac{1 - |\lambda|^2}{1 + |\lambda|^2} \cos(\Delta m_s \hat{t}) - \frac{2|\lambda| \sin \phi_s}{1 + |\lambda|^2} \sin(\Delta m_s \hat{t}) \right], \quad (3)$$

$$\bar{\Gamma}(\hat{t}) = \left| \frac{p}{q} \right|^2 \mathcal{N} e^{-\Gamma_s \hat{t}} \left[\cosh\left(\frac{\Delta\Gamma_s}{2}\hat{t}\right) - \frac{2|\lambda| \cos \phi_s}{1 + |\lambda|^2} \sinh\left(\frac{\Delta\Gamma_s}{2}\hat{t}\right) - \frac{1 - |\lambda|^2}{1 + |\lambda|^2} \cos(\Delta m_s \hat{t}) + \frac{2|\lambda| \sin \phi_s}{1 + |\lambda|^2} \sin(\Delta m_s \hat{t}) \right], \quad (4)$$

where $\Gamma_s \equiv (\Gamma_L + \Gamma_H)/2$ is the average decay width of the light and heavy mass eigenstates, $\Delta\Gamma_s \equiv \Gamma_L - \Gamma_H$ is their decay width difference and $\Delta m_s \equiv m_H - m_L$ is their mass difference. As Δm_s is large [28] and the production asymmetry is small [29], the effect of the production asymmetry is negligible and so the constant \mathcal{N} is the same for both B_s^0 and \bar{B}_s^0 mesons. Similarly we do not consider a tagging asymmetry in the fit as this is known to be consistent with zero. CP violation in mixing and decay is parameterised by the factor $\lambda \equiv \frac{q \bar{A}_f}{p A_f}$, with $\phi_s \equiv -\arg(\lambda)$. The terms A_f (\bar{A}_f) are the amplitudes for the B_s^0 (\bar{B}_s^0) decay to the final state f , which in this case is $f = D_s^+ D_s^-$, and the complex parameters $p = \langle B_s^0 | B_L \rangle$ and $q = \langle \bar{B}_s^0 | B_L \rangle$ relate the mass and flavour eigenstates. The factor $|p/q|^2$ in Eq. (4) is related to the flavour-specific CP asymmetry, a_{sl}^s , by

$$a_{\text{sl}}^s = \frac{|p/q|^2 - |q/p|^2}{|p/q|^2 + |q/p|^2} \approx |p/q|^2 - 1. \quad (5)$$

LHCb has measured $a_{\text{sl}}^s = (-0.06 \pm 0.50 \text{ (stat)} \pm 0.36 \text{ (syst)})\%$ [30], implying $|p/q|^2 = 0.9994 \pm 0.0062$. We assume that it is unity in this analysis and that any observed deviation of $|\lambda|$ from 1 is due to CP violation in the decay, *i.e.* $|\bar{A}_f/A_f| \neq 1$.

The initial flavor of the signal b hadron is determined using two methods. In hadron collisions, b hadrons are mostly produced as pairs: the opposite-side (OS) tagger [31]

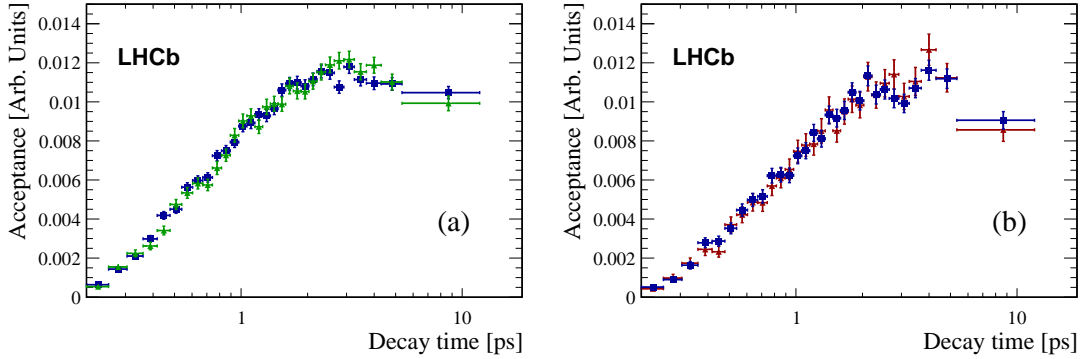


Figure 2: Decay time acceptances in simulation and data: (a) the $B^0 \rightarrow D^- D_s^+$ acceptance in data (green triangles) and simulation (blue squares), (b) the $\bar{B}_s^0 \rightarrow D_s^+ D_s^-$ acceptance in simulation (blue squares) and the $B^0 \rightarrow D^- D_s^+$ acceptance corrected for $\bar{B}_s^0 \rightarrow D_s^+ D_s^-$ (red triangles). The correction is described in detail in the text.

determines the flavour of the other b hadron in the event by identifying the charges of the leptons and kaons into which it decays, or the net charge of particles forming a detached vertex consistent with that of a b hadron. The neural network same-side (SS) kaon tagger [4] exploits the hadronisation process in which the fragmentation of a $\bar{b}(b)$ into a $B_s^0(\bar{B}_s^0)$ meson leads to an extra $\bar{s}(s)$ quark, which often forms a $K^+(K^-)$ meson, the charge of which identifies the initial \bar{B}_s^0 flavour. The SS kaon tagger uses an improved algorithm with respect to Ref. [4] that enhances the fraction of correctly tagged mesons by 40%. In both tagging algorithms a per-event wrong-tag probability estimate, η^{tag} , is determined, based on the output of a neural network trained on either simulated $\bar{B}_s^0 \rightarrow D_s^+ \pi^-$ events for the SS tagger, or, in the case of the OS algorithm, using a data sample of $B^- \rightarrow J/\psi K^-$ decays. The taggers are then calibrated in data using flavour-specific decay modes in order to provide a per-event wrong-tag probability, $\bar{\omega}(\eta^{\text{tag}})$, for an initial flavour \bar{B}_s^0 meson. The calibration is performed separately for the two tagging algorithms, which are then combined in the fit. The effective tagging power is parameterised by $\varepsilon_{\text{tag}} D^2$ where $D \equiv (1 - 2\bar{\omega})$ and ε_{tag} is the fraction events tagged by the algorithm.

The combined effective tagging power is $\varepsilon_{\text{tag}} D^2 = (5.33 \pm 0.18 \text{ (stat)} \pm 0.17 \text{ (syst)})\%$, comparable to that of other recent analyses [32]. The rate expression including flavour tagging is

$$R(\hat{t}, q^{\text{OS}} | \eta^{\text{OS}}, q^{\text{SS}} | \eta^{\text{SS}}) = (1 + q^{\text{OS}}[1 - 2\bar{\omega}^{\text{OS}}])(1 + q^{\text{SS}}[1 - 2\bar{\omega}^{\text{SS}}])\Gamma(\hat{t}) + (1 - q^{\text{OS}}[1 - 2\bar{\omega}^{\text{OS}}])(1 - q^{\text{SS}}[1 - 2\bar{\omega}^{\text{SS}}])\bar{\Gamma}(\hat{t}). \quad (6)$$

The track reconstruction, trigger and selection efficiencies vary as a function of decay time, requiring that an acceptance function is included in the fit. The $\bar{B}_s^0 \rightarrow D_s^+ D_s^-$

acceptance is determined using

$$\varepsilon_{\text{data}}^{D_s^+ D_s^-}(t) = \varepsilon_{\text{data}}^{D^- D_s^+}(t) \times \frac{\varepsilon_{\text{sim}}^{D_s^+ D_s^-}(t)}{\varepsilon_{\text{sim}}^{D^- D_s^+}(t)}, \quad (7)$$

where $\varepsilon_{\text{data}}^{D^- D_s^+}(t)$ is the efficiency associated with the $B^0 \rightarrow D^- D_s^+$ control channel as determined directly from the data and $\varepsilon_{\text{sim}}^{D_s^+ D_s^-}/\varepsilon_{\text{sim}}^{D^- D_s^+}(t)$ is the relative efficiency obtained from simulation after all selections are applied. This correction accounts for the differences in lifetime as well as small kinematic differences between the signal and control channels. The first factor in Eq. (7) is

$$\varepsilon_{\text{data}}^{D^- D_s^+}(t) = \frac{N_{\text{data}}^{D^- D_s^+}(t)}{\mathcal{N} e^{-\Gamma_d \hat{t}} \otimes G(t - \hat{t} | \sigma_{\text{eff}})}, \quad (8)$$

where $N_{\text{data}}^{D^- D_s^+}(t)$ denotes the number of $B^0 \rightarrow D^- D_s^+$ signal decays in a given bin of the decay time distribution, $\mathcal{N} e^{-\Gamma_d \hat{t}}$ is an exponential with decay width equal to that of the world average value for B^0 mesons [17], \mathcal{N} is a constant and $G(t - \hat{t} | \sigma_{\text{eff}})$ is a Gaussian resolution function with width $\sigma_{\text{eff}} = 54$ fs, determined from simulation. In the fit, the acceptance is implemented as a histogram. The binning scheme is chosen to maintain approximately equal statistical power in each bin. Figure 2(a) shows $\varepsilon_{\text{data}}^{D^- D_s^+}(t)$ and $\varepsilon_{\text{sim}}^{D^- D_s^+}(t)$, while Fig. 2(b) shows $\varepsilon_{\text{sim}}^{D_s^+ D_s^-}(t)$ and $\varepsilon_{\text{data}}^{D_s^+ D_s^-}(t)$ as used in the fit to extract ϕ_s . The procedure is verified by fitting for the decay width in both the signal and the control channels, where the results are found to be consistent with the published values.

The fit to determine ϕ_s uses a decay time uncertainty estimated in each event and obtained from the constrained vertex fit from which the decay time is determined. The resolution function is

$$G(t - \hat{t} | \delta) = \frac{1}{\sqrt{2\pi}\sigma(\delta)} e^{-\frac{1}{2}\left(\frac{t-\hat{t}}{\sigma(\delta)}\right)^2}. \quad (9)$$

The per-event resolution, $\sigma(\delta)$, is calibrated using simulated signal decays by fitting the effective resolution, σ_{eff} , in bins of the per-event decay time error estimate, $\sigma_{\text{eff}} = q_0 + q_1\delta$. The effective resolution is determined by fitting to the event-by-event decay time difference between the reconstructed and generated decay time in simulated signal decays. The effective resolution is the sum in quadrature of the widths of two Gaussian functions contributing with their corresponding fractions. The values $q_0 = 8.9 \pm 1.3$ fs and $q_1 = 1.014 \pm 0.036$ are obtained from the fit, resulting in a calibrated effective resolution of 54 fs.

In the fits that determine ϕ_s , we apply Gaussian constraints to the average decay width, $\Gamma_s = 0.661 \pm 0.007$ ps⁻¹, the decay width difference, $\Delta\Gamma_s = 0.106 \pm 0.013$ ps⁻¹ [4], the mixing frequency, $\Delta m_s = 17.168 \pm 0.024$ ps⁻¹ [28] and the flavour tagging and resolution calibration parameters. The correlation between Γ_s and $\Delta\Gamma_s$ is accounted for in the fit. Two fits to the data are performed, one assuming no CP violation in decay, *i.e.* $|\lambda| = 1$, and a second where this assumption is removed. The fit is validated using pseudoexperiments and simulated LHCb events.

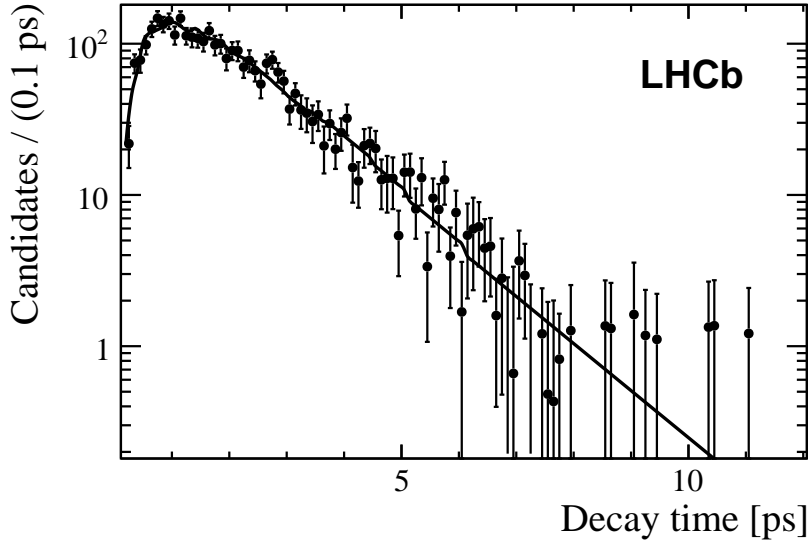


Figure 3: Distribution of the decay time for $\bar{B}_s^0 \rightarrow D_s^+ D_s^-$ signal decays with background subtracted using the *sPlot* method, along with the fit as described in the text. Discontinuities in the fit line shape are a result of the binned acceptance.

Table 1: Summary of systematic uncertainties not already accounted for in the fit, where σ denotes the statistical uncertainty.

Systematic uncertainty	ϕ_s ($ \lambda = 1$)	ϕ_s	$ \lambda $
Resolution	$\pm 0.098 \sigma$	$\pm 0.094 \sigma$	$\pm 0.100 \sigma$
Mass	$\pm 0.044 \sigma$	$\pm 0.043 \sigma$	$\pm 0.010 \sigma$
Acceptance (model)	$\pm 0.022 \sigma$	$\pm 0.027 \sigma$	$\pm 0.027 \sigma$
Acceptance (stat.)	$\pm 0.013 \sigma$	$\pm 0.013 \sigma$	$\pm 0.014 \sigma$
Background subtraction	$\pm 0.009 \sigma$	$\pm 0.008 \sigma$	$\pm 0.046 \sigma$
Total	$\pm 0.11 \sigma$	$\pm 0.11 \sigma$	$\pm 0.11 \sigma$

The systematic uncertainties on ϕ_s and $|\lambda|$ that are not accounted for by the use of Gaussian constraints are summarised in Table 1. The systematic uncertainty associated with the resolution calibration in simulated events is studied by generating pseudoexperiments with an alternative resolution parameterisation ($q_0 = 0$, $q_1 \in [1.25, 1.45]$ [28]) obtained in \bar{B}_s^0 decays in data. The effect of mismodelling of the mass PDF is studied by fitting using a larger mass window and including an additional background component from $\bar{B}_s^0 \rightarrow D_s^{*+} D_s^{*-}$. The effect of mismodelling the acceptance distribution is studied by fitting the $\bar{B}_s^0 \rightarrow D_s^+ D_s^-$ derived acceptance in pseudoexperiments generated with the acceptance distribution determined entirely from $\bar{B}_s^0 \rightarrow D_s^+ D_s^-$ simulation. The uncertainty due to the finite size of the simulated data samples used to determine the acceptance correction is evaluated by fitting to the data 500 times with Gaussian fluctuations around the bin values with a width equal to the statistical uncertainties. We evaluate the uncertainty due

to the use of the *sPlot* method for background subtraction by fitting to simulated events, once with only signal candidates, and again to the *sPlot* determined from a mass fit to a sample containing the signal and background in proportions determined from data.

Assuming no *CP* violation in decay, we find

$$\phi_s = 0.02 \pm 0.17 \text{ (stat)} \pm 0.02 \text{ (syst)} \text{ rad},$$

where the first uncertainty is statistical and the second is systematic. In a fit to the same data in which we allow for the presence of *CP* violation in decay we find

$$\phi_s = 0.02 \pm 0.17 \text{ (stat)} \pm 0.02 \text{ (syst)} \text{ rad}, \quad |\lambda| = 0.91^{+0.18}_{-0.15} \text{ (stat)} \pm 0.02 \text{ (syst)},$$

where ϕ_s and $|\lambda|$ have a correlation coefficient of 3%. This measurement is consistent with no *CP* violation. The decay time distribution and the corresponding fit projection for the case where *CP* violation in decay is allowed are shown in Fig. 3.

In conclusion, we present the first analysis of the time evolution of flavour-tagged $\bar{B}_s^0 \rightarrow D_s^+ D_s^-$ decays. We measure the *CP*-violating weak phase ϕ_s , allowing for the presence of *CP* violation in decay, and find that it is consistent with the Standard Model expectation and with measurements of ϕ_s in other decay modes.

Acknowledgements

We express our gratitude to our colleagues in the CERN accelerator departments for the excellent performance of the LHC. We thank the technical and administrative staff at the LHCb institutes. We acknowledge support from CERN and from the national agencies: CAPES, CNPq, FAPERJ and FINEP (Brazil); NSFC (China); CNRS/IN2P3 (France); BMBF, DFG, HGF and MPG (Germany); SFI (Ireland); INFN (Italy); FOM and NWO (The Netherlands); MNiSW and NCN (Poland); MEN/IFA (Romania); MinES and FANO (Russia); MinECo (Spain); SNSF and SER (Switzerland); NASU (Ukraine); STFC (United Kingdom); NSF (USA). The Tier1 computing centres are supported by IN2P3 (France), KIT and BMBF (Germany), INFN (Italy), NWO and SURF (The Netherlands), PIC (Spain), GridPP (United Kingdom). We are indebted to the communities behind the multiple open source software packages on which we depend. We are also thankful for the computing resources and the access to software R&D tools provided by Yandex LLC (Russia). Individual groups or members have received support from EPLANET, Marie Skłodowska-Curie Actions and ERC (European Union), Conseil général de Haute-Savoie, Labex ENIGMASS and OCEVU, Région Auvergne (France), RFBR (Russia), XuntaGal and GENCAT (Spain), Royal Society and Royal Commission for the Exhibition of 1851 (United Kingdom).

References

- [1] J. Charles *et al.*, *Predictions of selected flavor observables within the Standard Model*, Phys. Rev. **D84** (2011) 033005, [arXiv:1106.4041](#).
- [2] CDF collaboration, T. Aaltonen *et al.*, *First flavor-tagged determination of bounds on mixing-induced CP violation in $B_s^0 \rightarrow J/\psi\phi$ decays*, Phys. Rev. Lett. **100** (2008) 161802, [arXiv:0712.2397](#).
- [3] D0 collaboration, V. M. Abazov *et al.*, *Measurement of B_s^0 mixing parameters from the flavor-tagged decay $B_s^0 \rightarrow J/\psi\phi$* , Phys. Rev. Lett. **101** (2008) 241801, [arXiv:0802.2255](#).
- [4] LHCb collaboration, R. Aaij *et al.*, *Measurement of CP violation and the B_s^0 meson decay width difference with $B_s^0 \rightarrow J/\psi K^+K^-$ and $B_s^0 \rightarrow J/\psi\pi^+\pi^-$ decays*, Phys. Rev. **D87** (2013) 112010, [arXiv:1304.2600](#).
- [5] LHCb collaboration, R. Aaij *et al.*, *Measurement of the CP violationg phase ϕ_s in $\bar{B}_s^0 \rightarrow J/\psi\pi^+\pi^-$ decays*, Phys. Lett. **B736** (2014) 186, [arXiv:1405.4140](#).
- [6] D0 Collaboration, V. M. Abazov *et al.*, *Measurement of the CP-violating phase $\phi_s^{J/\psi\phi}$ using the flavor-tagged decay $B_s^0 \rightarrow J/\psi\phi$ in 8 fb^{-1} of $p\bar{p}$ collisions*, Phys. Rev. **D85** (2012) 032006, [arXiv:1109.3166](#).
- [7] ATLAS collaboration, G. Aad *et al.*, *Time-dependent angular analysis of the decay $B_s^0 \rightarrow J/\psi\phi$ and extraction of $\Delta\Gamma_s$ and the CP-violating weak phase ϕ_s by ATLAS*, JHEP **12** (2012) 072, [arXiv:1208.0572](#).
- [8] CDF collaboration, T. Aaltonen *et al.*, *Measurement of the bottom-strange meson mixing phase in the full CDF data set*, Phys. Rev. Lett. **109** (2012) 171802, [arXiv:1208.2967](#).
- [9] Heavy Flavor Averaging Group, Y. Amhis *et al.*, *Averages of b-hadron, c-hadron, and τ -lepton properties as of early 2012*, [arXiv:1207.1158](#), updated results and plots available at <http://www.slac.stanford.edu/xorg/hfag/>.
- [10] S. Faller, R. Fleischer, and T. Mannel, *Precision physics with $B_s^0 \rightarrow J/\psi\phi$ at the LHC: The quest for new physics*, Phys. Rev. **D79** (2009) 014005, [arXiv:0810.4248](#).
- [11] R. Fleischer, *Exploring CP violation and penguin effects through $B_d^0 \rightarrow D^+D^-$ and $B_s^0 \rightarrow D_s^+D_s^-$* , Eur. Phys. J. **C51** (2007) 849, [arXiv:0705.4421](#).
- [12] I. Dunietz, R. Fleischer, and U. Nierste, *In pursuit of new physics with B_s decays*, Phys. Rev. **D63** (2001) 114015, [arXiv:hep-ph/0012219](#).
- [13] LHCb collaboration, A. A. Alves Jr. *et al.*, *The LHCb detector at the LHC*, JINST **3** (2008) S08005.

- [14] R. Aaij *et al.*, *The LHCb trigger and its performance in 2011*, JINST **8** (2013) P04022, [arXiv:1211.3055](#).
- [15] V. V. Gligorov and M. Williams, *Efficient, reliable and fast high-level triggering using a bonsai boosted decision tree*, JINST **8** (2013) P02013, [arXiv:1210.6861](#).
- [16] LHCb collaboration, R. Aaij *et al.*, *Measurement of the $\bar{B}_s^0 \rightarrow D_s^- D_s^+$ and $\bar{B}_s^0 \rightarrow D^- D_s^+$ effective lifetimes*, Phys. Rev. Lett. **112** (2014) 111802, [arXiv:1312.1217](#).
- [17] Particle Data Group, K. A. Olive *et al.*, *Review of particle physics*, Chin. Phys. **C38** (2014) 090001.
- [18] LHCb collaboration, R. Aaij *et al.*, *First observations of $\bar{B}_s^0 \rightarrow D^+ D^-$, $D_s^+ D^-$ and $D^0 \bar{D}^0$ decays*, Phys. Rev. **D87** (2013) 092007, [arXiv:1302.5854](#).
- [19] W. D. Hulsbergen, *Decay chain fitting with a Kalman filter*, Nucl. Instrum. Meth. **A552** (2005) 566, [arXiv:physics/0503191](#).
- [20] L. Breiman, J. H. Friedman, R. A. Olshen, and C. J. Stone, *Classification and regression trees*, Wadsworth international group, Belmont, California, USA, 1984.
- [21] R. E. Schapire and Y. Freund, *A decision-theoretic generalization of on-line learning and an application to boosting*, Jour. Comp. and Syst. Sc. **55** (1997) 119.
- [22] T. Sjöstrand, S. Mrenna, and P. Skands, *PYTHIA 6.4 physics and manual*, JHEP **05** (2006) 026, [arXiv:hep-ph/0603175](#); I. Belyaev *et al.*, *Handling of the generation of primary events in Gauss, the LHCb simulation framework*, Nuclear Science Symposium Conference Record (NSS/MIC) IEEE (2010) 1155.
- [23] D. J. Lange, *The EvtGen particle decay simulation package*, Nucl. Instrum. Meth. **A462** (2001) 152.
- [24] P. Golonka and Z. Was, *PHOTOS Monte Carlo: A precision tool for QED corrections in Z and W decays*, Eur. Phys. J. **C45** (2006) 97, [arXiv:hep-ph/0506026](#).
- [25] Geant4 collaboration, J. Allison *et al.*, *Geant4 developments and applications*, IEEE Trans. Nucl. Sci. **53** (2006) 270; Geant4 collaboration, S. Agostinelli *et al.*, *Geant4: a simulation toolkit*, Nucl. Instrum. Meth. **A506** (2003) 250; M. Clemencic *et al.*, *The LHCb simulation application, Gauss: Design, evolution and experience*, J. Phys. Conf. Ser. **331** (2011) 032023.
- [26] M. Pivk and F. R. Le Diberder, *sPlot: A statistical tool to unfold data distributions*, Nucl. Instrum. Meth. **A555** (2005) 356, [arXiv:physics/0402083](#).
- [27] Y. Xie, *sFit: A method for background subtraction in maximum likelihood fit*, [arXiv:0905.0724](#).

- [28] LHCb collaboration, R. Aaij *et al.*, *Precision measurement of the $B_s^0 - \bar{B}_s^0$ oscillation frequency in the decay $B_s^0 \rightarrow D_s^- \pi^+$* , New J. Phys. **15** (2013) 053021, [arXiv:1304.4741](https://arxiv.org/abs/1304.4741).
- [29] LHCb collaboration, R. Aaij *et al.*, *Measurement of the $\bar{B}^0 - B^0$ and $\bar{B}_s^0 - B_s^0$ production asymmetries in pp collisions at $\sqrt{s} = 7$ TeV*, [arXiv:1408.0275](https://arxiv.org/abs/1408.0275), submitted to Phys. Lett. B.
- [30] LHCb collaboration, R. Aaij *et al.*, *Measurement of the flavour-specific CP-violating asymmetry a_{sl}^s in B_s^0 decays*, Phys. Lett. **B728** (2014) 607, [arXiv:1308.1048](https://arxiv.org/abs/1308.1048).
- [31] LHCb collaboration, R. Aaij *et al.*, *Opposite-side flavour tagging of B mesons at the LHCb experiment*, Eur. Phys. J. **C72** (2012) 2022, [arXiv:1202.4979](https://arxiv.org/abs/1202.4979).
- [32] LHCb collaboration, R. Aaij *et al.*, *Measurement of CP asymmetry in $B_s^0 \rightarrow D_s^\mp K^\pm$ decays*, [arXiv:1407.6127](https://arxiv.org/abs/1407.6127), submitted to JHEP.

LHCb collaboration

R. Aaij⁴¹, C. Abellán Beteta⁴⁰, B. Adeva³⁷, M. Adinolfi⁴⁶, A. Affolder⁵², Z. Ajaltouni⁵, S. Akar⁶, J. Albrecht⁹, F. Alessio³⁸, M. Alexander⁵¹, S. Ali⁴¹, G. Alkhazov³⁰, P. Alvarez Cartelle³⁷, A.A. Alves Jr^{25,38}, S. Amato², S. Amerio²², Y. Amhis⁷, L. An³, L. Anderlini^{17,g}, J. Anderson⁴⁰, R. Andreassen⁵⁷, M. Andreotti^{16,f}, J.E. Andrews⁵⁸, R.B. Appleby⁵⁴, O. Aquines Gutierrez¹⁰, F. Archilli³⁸, A. Artamonov³⁵, M. Artuso⁵⁹, E. Aslanides⁶, G. Auriemma^{25,n}, M. Baalouch⁵, S. Bachmann¹¹, J.J. Back⁴⁸, A. Badalov³⁶, C. Baesso⁶⁰, W. Baldini¹⁶, R.J. Barlow⁵⁴, C. Barschel³⁸, S. Barsuk⁷, W. Barter⁴⁷, V. Batozskaya²⁸, V. Battista³⁹, A. Bay³⁹, L. Beaucourt⁴, J. Beddow⁵¹, F. Bedeschi²³, I. Bediaga¹, S. Belogurov³¹, K. Belous³⁵, I. Belyaev³¹, E. Ben-Haim⁸, G. Bencivenni¹⁸, S. Benson³⁸, J. Benton⁴⁶, A. Berezhnoy³², R. Bernet⁴⁰, M.-O. Bettler⁴⁷, M. van Beuzekom⁴¹, A. Bien¹¹, S. Bifani⁴⁵, T. Bird⁵⁴, A. Bizzeti^{17,i}, P.M. Bjørnstad⁵⁴, T. Blake⁴⁸, F. Blanc³⁹, J. Blouw¹⁰, S. Blusk⁵⁹, V. Bocci²⁵, A. Bondar³⁴, N. Bondar^{30,38}, W. Bonivento^{15,38}, S. Borghi⁵⁴, A. Borgia⁵⁹, M. Borsato⁷, T.J.V. Bowcock⁵², E. Bowen⁴⁰, C. Bozzi¹⁶, T. Brambach⁹, D. Brett⁵⁴, M. Britsch¹⁰, T. Britton⁵⁹, J. Brodzicka⁵⁴, N.H. Brook⁴⁶, H. Brown⁵², A. Bursche⁴⁰, G. Busetto^{22,r}, J. Buytaert³⁸, S. Cadeddu¹⁵, R. Calabrese^{16,f}, M. Calvi^{20,k}, M. Calvo Gomez^{36,p}, P. Campana¹⁸, D. Campora Perez³⁸, A. Carbone^{14,d}, G. Carboni^{24,l}, R. Cardinale^{19,38,j}, A. Cardini¹⁵, L. Carson⁵⁰, K. Carvalho Akiba², G. Casse⁵², L. Cassina²⁰, L. Castillo Garcia³⁸, M. Cattaneo³⁸, Ch. Cauet⁹, R. Cenci⁵⁸, M. Charles⁸, Ph. Charpentier³⁸, M. Chefdeville⁴, S. Chen⁵⁴, S.-F. Cheung⁵⁵, N. Chiapolini⁴⁰, M. Chrzaszcz^{40,26}, X. Cid Vidal³⁸, G. Ciezarek⁵³, P.E.L. Clarke⁵⁰, M. Clemencic³⁸, H.V. Cliff⁴⁷, J. Closier³⁸, V. Coco³⁸, J. Cogan⁶, E. Cogneras⁵, V. Cogoni¹⁵, L. Cojocariu²⁹, P. Collins³⁸, A. Comerma-Montells¹¹, A. Contu^{15,38}, A. Cook⁴⁶, M. Coombes⁴⁶, S. Coquereau⁸, G. Corti³⁸, M. Corvo^{16,f}, I. Counts⁵⁶, B. Couturier³⁸, G.A. Cowan⁵⁰, D.C. Craik⁴⁸, M. Cruz Torres⁶⁰, S. Cunliffe⁵³, R. Currie⁵⁰, C. D'Ambrosio³⁸, J. Dalseno⁴⁶, P. David⁸, P.N.Y. David⁴¹, A. Davis⁵⁷, K. De Bruyn⁴¹, S. De Capua⁵⁴, M. De Cian¹¹, J.M. De Miranda¹, L. De Paula², W. De Silva⁵⁷, P. De Simone¹⁸, D. Decamp⁴, M. Deckenhoff⁹, L. Del Buono⁸, N. Déléage⁴, D. Derkach⁵⁵, O. Deschamps⁵, F. Dettori³⁸, A. Di Canto³⁸, H. Dijkstra³⁸, S. Donleavy⁵², F. Dordei¹¹, M. Dorigo³⁹, A. Dosil Suárez³⁷, D. Dossett⁴⁸, A. Dovbnya⁴³, K. Dreimanis⁵², G. Dujany⁵⁴, F. Dupertuis³⁹, P. Durante³⁸, R. Dzhelyadin³⁵, A. Dziurda²⁶, A. Dzyuba³⁰, S. Easo^{49,38}, U. Egede⁵³, V. Egorychev³¹, S. Eidelman³⁴, S. Eisenhardt⁵⁰, U. Eitschberger⁹, R. Ekelhof⁹, L. Eklund⁵¹, I. El Rifai⁵, E. Elena⁴⁰, Ch. Elsasser⁴⁰, S. Ely⁵⁹, S. Esen¹¹, H.-M. Evans⁴⁷, T. Evans⁵⁵, A. Falabella¹⁴, C. Färber¹¹, C. Farinelli⁴¹, N. Farley⁴⁵, S. Farry⁵², RF Fay⁵², D. Ferguson⁵⁰, V. Fernandez Albor³⁷, F. Ferreira Rodrigues¹, M. Ferro-Luzzi³⁸, S. Filippov³³, M. Fiore^{16,f}, M. Fiorini^{16,f}, M. Firlej²⁷, C. Fitzpatrick³⁹, T. Fiutowski²⁷, P. Fol⁵³, M. Fontana¹⁰, F. Fontanelli^{19,j}, R. Forty³⁸, O. Francisco², M. Frank³⁸, C. Frei³⁸, M. Frosini^{17,g}, J. Fu^{21,38}, E. Furfaro^{24,l}, A. Gallas Torreira³⁷, D. Galli^{14,d}, S. Gallorini^{22,38}, S. Gambetta^{19,j}, M. Gandelman², P. Gandini⁵⁹, Y. Gao³, J. García Pardiñas³⁷, J. Garofoli⁵⁹, J. Garra Tico⁴⁷, L. Garrido³⁶, C. Gaspar³⁸, R. Gauld⁵⁵, L. Gavardi⁹, G. Gavrilov³⁰, A. Geraci^{21,v}, E. Gersabeck¹¹, M. Gersabeck⁵⁴, T. Gershon⁴⁸, Ph. Ghez⁴, A. Gianelle²², S. Gianì³⁹, V. Gibson⁴⁷, L. Giubega²⁹, V.V. Gligorov³⁸, C. Göbel⁶⁰, D. Golubkov³¹, A. Golutvin^{53,31,38}, A. Gomes^{1,a}, C. Gotti²⁰, M. Grabalosa Gándara⁵, R. Graciani Diaz³⁶, L.A. Granado Cardoso³⁸, E. Graugés³⁶, G. Graziani¹⁷, A. Grecu²⁹, E. Greening⁵⁵, S. Gregson⁴⁷, P. Griffith⁴⁵, L. Grillo¹¹, O. Grünberg⁶², B. Gui⁵⁹, E. Gushchin³³, Yu. Guz^{35,38}, T. Gys³⁸, C. Hadjivasiliou⁵⁹, G. Haefeli³⁹, C. Haen³⁸, S.C. Haines⁴⁷, S. Hall⁵³, B. Hamilton⁵⁸, T. Hampson⁴⁶, X. Han¹¹, S. Hansmann-Menzemer¹¹,

N. Harnew⁵⁵, S.T. Harnew⁴⁶, J. Harrison⁵⁴, J. He³⁸, T. Head³⁸, V. Heijne⁴¹, K. Hennessy⁵², P. Henrard⁵, L. Henry⁸, J.A. Hernando Morata³⁷, E. van Herwijnen³⁸, M. Hef⁶², A. Hicheur², D. Hill⁵⁵, M. Hoballah⁵, C. Hombach⁵⁴, W. Hulsbergen⁴¹, P. Hunt⁵⁵, N. Hussain⁵⁵, D. Hutchcroft⁵², D. Hynds⁵¹, M. Idzik²⁷, P. Ilten⁵⁶, R. Jacobsson³⁸, A. Jaeger¹¹, J. Jalocha⁵⁵, E. Jans⁴¹, P. Jaton³⁹, A. Jawahery⁵⁸, F. Jing³, M. John⁵⁵, D. Johnson³⁸, C.R. Jones⁴⁷, C. Joram³⁸, B. Jost³⁸, N. Jurik⁵⁹, M. Kaballo⁹, S. Kandybei⁴³, W. Kanso⁶, M. Karacson³⁸, T.M. Karbach³⁸, S. Karodia⁵¹, M. Kelsey⁵⁹, I.R. Kenyon⁴⁵, T. Ketel⁴², B. Khanji^{20,38}, C. Khurewathanakul³⁹, S. Klaver⁵⁴, K. Klimaszewski²⁸, O. Kochebina⁷, M. Kolpin¹¹, I. Komarov³⁹, R.F. Koopman⁴², P. Koppenburg^{41,38}, M. Korolev³², A. Kozlinskiy⁴¹, L. Kravchuk³³, K. Kreplin¹¹, M. Kreps⁴⁸, G. Krocker¹¹, P. Krokovny³⁴, F. Kruse⁹, W. Kucewicz^{26,o}, M. Kucharczyk^{20,26,k}, V. Kudryavtsev³⁴, K. Kurek²⁸, T. Kvaratskheliya³¹, V.N. La Thi³⁹, D. Lacarrere³⁸, G. Lafferty⁵⁴, A. Lai¹⁵, D. Lambert⁵⁰, R.W. Lambert⁴², G. Lanfranchi¹⁸, C. Langenbruch⁴⁸, B. Langhans³⁸, T. Latham⁴⁸, C. Lazzeroni⁴⁵, R. Le Gac⁶, J. van Leerdam⁴¹, J.-P. Lees⁴, R. Lefevre⁵, A. Leflat³², J. Lefrançois⁷, S. Leo²³, O. Leroy⁶, T. Lesiak²⁶, B. Leverington¹¹, Y. Li³, T. Likhomanenko⁶³, M. Liles⁵², R. Lindner³⁸, C. Linn³⁸, F. Lionetto⁴⁰, B. Liu¹⁵, S. Lohn³⁸, I. Longstaff⁵¹, J.H. Lopes², N. Lopez-March³⁹, P. Lowdon⁴⁰, D. Lucchesi^{22,r}, H. Luo⁵⁰, A. Lupato²², E. Luppi^{16,f}, O. Lupton⁵⁵, F. Machefert⁷, I.V. Machikhiliyan³¹, F. Maciuc²⁹, O. Maev³⁰, S. Malde⁵⁵, A. Malinin⁶³, G. Manca^{15,e}, G. Mancinelli⁶, A. Mapelli³⁸, J. Maratas⁵, J.F. Marchand⁴, U. Marconi¹⁴, C. Marin Benito³⁶, P. Marino^{23,t}, R. Märki³⁹, J. Marks¹¹, G. Martellotti²⁵, A. Martín Sánchez⁷, M. Martinelli³⁹, D. Martinez Santos^{42,38}, F. Martinez Vidal⁶⁴, D. Martins Tostes², A. Massafferri¹, R. Matev³⁸, Z. Mathe³⁸, C. Matteuzzi²⁰, A. Mazurov⁴⁵, M. McCann⁵³, J. McCarthy⁴⁵, A. McNab⁵⁴, R. McNulty¹², B. McSkelly⁵², B. Meadows⁵⁷, F. Meier⁹, M. Meissner¹¹, M. Merk⁴¹, D.A. Milanes⁸, M.-N. Minard⁴, N. Moggi¹⁴, J. Molina Rodriguez⁶⁰, S. Monteil⁵, M. Morandin²², P. Morawski²⁷, A. Mordà⁶, M.J. Morello^{23,t}, J. Moron²⁷, A.-B. Morris⁵⁰, R. Mountain⁵⁹, F. Muheim⁵⁰, K. Müller⁴⁰, M. Mussini¹⁴, B. Muster³⁹, P. Naik⁴⁶, T. Nakada³⁹, R. Nandakumar⁴⁹, I. Nasteva², M. Needham⁵⁰, N. Neri²¹, S. Neubert³⁸, N. Neufeld³⁸, M. Neuner¹¹, A.D. Nguyen³⁹, T.D. Nguyen³⁹, C. Nguyen-Mau^{39,q}, M. Nicol⁷, V. Niess⁵, R. Niet⁹, N. Nikitin³², T. Nikodem¹¹, A. Novoselov³⁵, D.P. O'Hanlon⁴⁸, A. Oblakowska-Mucha^{27,38}, V. Obraztsov³⁵, S. Oggero⁴¹, S. Ogilvy⁵¹, O. Okhrimenko⁴⁴, R. Oldeman^{15,e}, G. Onderwater⁶⁵, M. Orlandea²⁹, J.M. Otalora Goicochea², A. Otto³⁸, P. Owen⁵³, A. Oyanguren⁶⁴, B.K. Pal⁵⁹, A. Palano^{13,c}, F. Palombo^{21,u}, M. Palutan¹⁸, J. Panman³⁸, A. Papanestis^{49,38}, M. Pappagallo⁵¹, L.L. Pappalardo^{16,f}, C. Parkes⁵⁴, C.J. Parkinson^{9,45}, G. Passaleva¹⁷, G.D. Patel⁵², M. Patel⁵³, C. Patrignani^{19,j}, A. Pazos Alvarez³⁷, A. Pearce⁵⁴, A. Pellegrino⁴¹, M. Pepe Altarelli³⁸, S. Perazzini^{14,d}, E. Perez Trigo³⁷, P. Perret⁵, M. Perrin-Terrin⁶, L. Pescatore⁴⁵, E. Pesen⁶⁶, K. Petridis⁵³, A. Petrolini^{19,j}, E. Picatoste Olloqui³⁶, B. Pietrzyk⁴, T. Pilar⁴⁸, D. Pinci²⁵, A. Pistone¹⁹, S. Playfer⁵⁰, M. Plo Casasus³⁷, F. Polci⁸, A. Poluektov^{48,34}, E. Polycarpo², A. Popov³⁵, D. Popov¹⁰, B. Popovici²⁹, C. Potterat², E. Price⁴⁶, J.D. Price⁵², J. Prisciandaro³⁹, A. Pritchard⁵², C. Prouve⁴⁶, V. Pugatch⁴⁴, A. Puig Navarro³⁹, G. Punzi^{23,s}, W. Qian⁴, B. Rachwal²⁶, J.H. Rademacker⁴⁶, B. Rakotomiaramanana³⁹, M. Rama¹⁸, M.S. Rangel², I. Raniuk⁴³, N. Rauschmayr³⁸, G. Raven⁴², F. Redi⁵³, S. Reichert⁵⁴, M.M. Reid⁴⁸, A.C. dos Reis¹, S. Ricciardi⁴⁹, S. Richards⁴⁶, M. Rihl³⁸, K. Rinnert⁵², V. Rives Molina³⁶, P. Robbe⁷, A.B. Rodrigues¹, E. Rodrigues⁵⁴, P. Rodriguez Perez⁵⁴, S. Roiser³⁸, V. Romanovsky³⁵, A. Romero Vidal³⁷, M. Rotondo²², J. Rouvinet³⁹, T. Ruf³⁸, H. Ruiz³⁶, P. Ruiz Valls⁶⁴, J.J. Saborido Silva³⁷, N. Sagidova³⁰, P. Sail⁵¹, B. Saitta^{15,e}, V. Salustino Guimaraes², C. Sanchez Mayordomo⁶⁴, B. Sanmartin Sedes³⁷, R. Santacesaria²⁵,

C. Santamarina Rios³⁷, E. Santovetti^{24,l}, A. Sarti^{18,m}, C. Satriano^{25,n}, A. Satta²⁴, D.M. Saunders⁴⁶, M. Savrie^{16,f}, D. Savrina^{31,32}, M. Schiller⁴², H. Schindler³⁸, M. Schlupp⁹, M. Schmelling¹⁰, B. Schmidt³⁸, O. Schneider³⁹, A. Schopper³⁸, M.-H. Schune⁷, R. Schwemmer³⁸, B. Sciascia¹⁸, A. Sciubba²⁵, M. Seco³⁷, A. Semennikov³¹, I. Sepp⁵³, N. Serra⁴⁰, J. Serrano⁶, L. Sestini²², P. Seyfert¹¹, M. Shapkin³⁵, I. Shapoval^{16,43,f}, Y. Shcheglov³⁰, T. Shears⁵², L. Shekhtman³⁴, V. Shevchenko⁶³, A. Shires⁹, R. Silva Coutinho⁴⁸, G. Simi²², M. Sirendi⁴⁷, N. Skidmore⁴⁶, I. Skillicorn⁵¹, T. Skwarnicki⁵⁹, N.A. Smith⁵², E. Smith^{55,49}, E. Smith⁵³, J. Smith⁴⁷, M. Smith⁵⁴, H. Snoek⁴¹, M.D. Sokoloff⁵⁷, F.J.P. Soler⁵¹, F. Soomro³⁹, D. Souza⁴⁶, B. Souza De Paula², B. Spaan⁹, P. Spradlin⁵¹, S. Sridharan³⁸, F. Stagni³⁸, M. Stahl¹¹, S. Stahl¹¹, O. Steinkamp⁴⁰, O. Stenyakin³⁵, S. Stevenson⁵⁵, S. Stoica²⁹, S. Stone⁵⁹, B. Storaci⁴⁰, S. Stracka²³, M. Straticiuc²⁹, U. Straumann⁴⁰, R. Stroili²², V.K. Subbiah³⁸, L. Sun⁵⁷, W. Sutcliffe⁵³, K. Swientek²⁷, S. Swientek⁹, V. Syropoulos⁴², M. Szczekowski²⁸, P. Szczypka^{39,38}, D. Szilard², T. Szumlak²⁷, S. T'Jampens⁴, M. Teklishyn⁷, G. Tellarini^{16,f}, F. Teubert³⁸, C. Thomas⁵⁵, E. Thomas³⁸, J. van Tilburg⁴¹, V. Tisserand⁴, M. Tobin³⁹, J. Todd⁵⁷, S. Tolk⁴², L. Tomassetti^{16,f}, D. Tonelli³⁸, S. Topp-Joergensen⁵⁵, N. Torr⁵⁵, E. Tournefier⁴, S. Tourneur³⁹, M.T. Tran³⁹, M. Tresch⁴⁰, A. Tsaregorodtsev⁶, P. Tsopelas⁴¹, N. Tuning⁴¹, M. Ubeda Garcia³⁸, A. Ukleja²⁸, A. Ustyuzhanin⁶³, U. Uwer¹¹, C. Vacca¹⁵, V. Vagnoni¹⁴, G. Valenti¹⁴, A. Vallier⁷, R. Vazquez Gomez¹⁸, P. Vazquez Regueiro³⁷, C. Vázquez Sierra³⁷, S. Vecchi¹⁶, J.J. Velthuis⁴⁶, M. Veltri^{17,h}, G. Veneziano³⁹, M. Vesterinen¹¹, B. Viaud⁷, D. Vieira², M. Vieites Diaz³⁷, X. Vilasis-Cardona^{36,p}, A. Vollhardt⁴⁰, D. Volyanskyy¹⁰, D. Voong⁴⁶, A. Vorobyev³⁰, V. Vorobyev³⁴, C. Voß⁶², H. Voss¹⁰, J.A. de Vries⁴¹, R. Waldi⁶², C. Wallace⁴⁸, R. Wallace¹², J. Walsh²³, S. Wandernoth¹¹, J. Wang⁵⁹, D.R. Ward⁴⁷, N.K. Watson⁴⁵, D. Websdale⁵³, M. Whitehead⁴⁸, J. Wicht³⁸, D. Wiedner¹¹, G. Wilkinson^{55,38}, M.P. Williams⁴⁵, M. Williams⁵⁶, H.W. Wilschut⁶⁵, F.F. Wilson⁴⁹, J. Wimberley⁵⁸, J. Wishahi⁹, W. Wislicki²⁸, M. Witek²⁶, G. Wormser⁷, S.A. Wotton⁴⁷, S. Wright⁴⁷, K. Wyllie³⁸, Y. Xie⁶¹, Z. Xing⁵⁹, Z. Xu³⁹, Z. Yang³, X. Yuan³, O. Yushchenko³⁵, M. Zangoli¹⁴, M. Zavertyaev^{10,b}, L. Zhang⁵⁹, W.C. Zhang¹², Y. Zhang³, A. Zhelezov¹¹, A. Zhokhov³¹, L. Zhong³.

¹Centro Brasileiro de Pesquisas Físicas (CBPF), Rio de Janeiro, Brazil

²Universidade Federal do Rio de Janeiro (UFRJ), Rio de Janeiro, Brazil

³Center for High Energy Physics, Tsinghua University, Beijing, China

⁴LAPP, Université de Savoie, CNRS/IN2P3, Annecy-Le-Vieux, France

⁵Clermont Université, Université Blaise Pascal, CNRS/IN2P3, LPC, Clermont-Ferrand, France

⁶CPPM, Aix-Marseille Université, CNRS/IN2P3, Marseille, France

⁷LAL, Université Paris-Sud, CNRS/IN2P3, Orsay, France

⁸LPNHE, Université Pierre et Marie Curie, Université Paris Diderot, CNRS/IN2P3, Paris, France

⁹Fakultät Physik, Technische Universität Dortmund, Dortmund, Germany

¹⁰Max-Planck-Institut für Kernphysik (MPIK), Heidelberg, Germany

¹¹Physikalisches Institut, Ruprecht-Karls-Universität Heidelberg, Heidelberg, Germany

¹²School of Physics, University College Dublin, Dublin, Ireland

¹³Sezione INFN di Bari, Bari, Italy

¹⁴Sezione INFN di Bologna, Bologna, Italy

¹⁵Sezione INFN di Cagliari, Cagliari, Italy

¹⁶Sezione INFN di Ferrara, Ferrara, Italy

¹⁷Sezione INFN di Firenze, Firenze, Italy

¹⁸Laboratori Nazionali dell'INFN di Frascati, Frascati, Italy

¹⁹Sezione INFN di Genova, Genova, Italy

²⁰Sezione INFN di Milano Bicocca, Milano, Italy

²¹Sezione INFN di Milano, Milano, Italy

- ²²Sezione INFN di Padova, Padova, Italy
²³Sezione INFN di Pisa, Pisa, Italy
²⁴Sezione INFN di Roma Tor Vergata, Roma, Italy
²⁵Sezione INFN di Roma La Sapienza, Roma, Italy
²⁶Henryk Niewodniczanski Institute of Nuclear Physics Polish Academy of Sciences, Kraków, Poland
²⁷AGH - University of Science and Technology, Faculty of Physics and Applied Computer Science, Kraków, Poland
²⁸National Center for Nuclear Research (NCBJ), Warsaw, Poland
²⁹Horia Hulubei National Institute of Physics and Nuclear Engineering, Bucharest-Magurele, Romania
³⁰Petersburg Nuclear Physics Institute (PNPI), Gatchina, Russia
³¹Institute of Theoretical and Experimental Physics (ITEP), Moscow, Russia
³²Institute of Nuclear Physics, Moscow State University (SINP MSU), Moscow, Russia
³³Institute for Nuclear Research of the Russian Academy of Sciences (INR RAN), Moscow, Russia
³⁴Budker Institute of Nuclear Physics (SB RAS) and Novosibirsk State University, Novosibirsk, Russia
³⁵Institute for High Energy Physics (IHEP), Protvino, Russia
³⁶Universitat de Barcelona, Barcelona, Spain
³⁷Universidad de Santiago de Compostela, Santiago de Compostela, Spain
³⁸European Organization for Nuclear Research (CERN), Geneva, Switzerland
³⁹Ecole Polytechnique Fédérale de Lausanne (EPFL), Lausanne, Switzerland
⁴⁰Physik-Institut, Universität Zürich, Zürich, Switzerland
⁴¹Nikhef National Institute for Subatomic Physics, Amsterdam, The Netherlands
⁴²Nikhef National Institute for Subatomic Physics and VU University Amsterdam, Amsterdam, The Netherlands
⁴³NSC Kharkiv Institute of Physics and Technology (NSC KIPT), Kharkiv, Ukraine
⁴⁴Institute for Nuclear Research of the National Academy of Sciences (KINR), Kyiv, Ukraine
⁴⁵University of Birmingham, Birmingham, United Kingdom
⁴⁶H.H. Wills Physics Laboratory, University of Bristol, Bristol, United Kingdom
⁴⁷Cavendish Laboratory, University of Cambridge, Cambridge, United Kingdom
⁴⁸Department of Physics, University of Warwick, Coventry, United Kingdom
⁴⁹STFC Rutherford Appleton Laboratory, Didcot, United Kingdom
⁵⁰School of Physics and Astronomy, University of Edinburgh, Edinburgh, United Kingdom
⁵¹School of Physics and Astronomy, University of Glasgow, Glasgow, United Kingdom
⁵²Oliver Lodge Laboratory, University of Liverpool, Liverpool, United Kingdom
⁵³Imperial College London, London, United Kingdom
⁵⁴School of Physics and Astronomy, University of Manchester, Manchester, United Kingdom
⁵⁵Department of Physics, University of Oxford, Oxford, United Kingdom
⁵⁶Massachusetts Institute of Technology, Cambridge, MA, United States
⁵⁷University of Cincinnati, Cincinnati, OH, United States
⁵⁸University of Maryland, College Park, MD, United States
⁵⁹Syracuse University, Syracuse, NY, United States
⁶⁰Pontifícia Universidade Católica do Rio de Janeiro (PUC-Rio), Rio de Janeiro, Brazil, associated to ²
⁶¹Institute of Particle Physics, Central China Normal University, Wuhan, Hubei, China, associated to ³
⁶²Institut für Physik, Universität Rostock, Rostock, Germany, associated to ¹¹
⁶³National Research Centre Kurchatov Institute, Moscow, Russia, associated to ³¹
⁶⁴Instituto de Fisica Corpuscular (IFIC), Universitat de Valencia-CSIC, Valencia, Spain, associated to ³⁶
⁶⁵KVI - University of Groningen, Groningen, The Netherlands, associated to ⁴¹
⁶⁶Celal Bayar University, Manisa, Turkey, associated to ³⁸

^aUniversidade Federal do Triângulo Mineiro (UFTM), Uberaba-MG, Brazil

^bP.N. Lebedev Physical Institute, Russian Academy of Science (LPI RAS), Moscow, Russia

^cUniversità di Bari, Bari, Italy

^dUniversità di Bologna, Bologna, Italy

- ^e Università di Cagliari, Cagliari, Italy
^f Università di Ferrara, Ferrara, Italy
^g Università di Firenze, Firenze, Italy
^h Università di Urbino, Urbino, Italy
ⁱ Università di Modena e Reggio Emilia, Modena, Italy
^j Università di Genova, Genova, Italy
^k Università di Milano Bicocca, Milano, Italy
^l Università di Roma Tor Vergata, Roma, Italy
^m Università di Roma La Sapienza, Roma, Italy
ⁿ Università della Basilicata, Potenza, Italy
^o AGH - University of Science and Technology, Faculty of Computer Science, Electronics and Telecommunications, Kraków, Poland
^p LIFAELS, La Salle, Universitat Ramon Llull, Barcelona, Spain
^q Hanoi University of Science, Hanoi, Viet Nam
^r Università di Padova, Padova, Italy
^s Università di Pisa, Pisa, Italy
^t Scuola Normale Superiore, Pisa, Italy
^u Università degli Studi di Milano, Milano, Italy
^v Politecnico di Milano, Milano, Italy